

Phase-space analysis for hydrodynamic traffic models

P. Saavedra¹ and R. M. Velasco²

¹*Department of Mathematics, Universidad Autónoma Metropolitana, Iztapalapa 09340, Mexico*

²*Department of Physics, Universidad Autónoma Metropolitana, Iztapalapa 09340, Mexico*

(Received 4 November 2008; published 9 June 2009)

This work is devoted to the study of steady states in two hydrodynamic traffic models. The first model to be analyzed is the Kerner-Konhäuser model and the second is called kinetic Navier-Stokes model. The study is made through an analysis in the phase space. Taking into account the analogy with the description of the one-particle motion, we can give a sensible meaning to the dynamical functions which determine the stability of the steady states. Lastly, we constructed the phase plane paths in several cases for both models.

DOI: [10.1103/PhysRevE.79.066103](https://doi.org/10.1103/PhysRevE.79.066103)

PACS number(s): 89.40.-a, 45.70.Vn, 47.90.+a

I. INTRODUCTION

Traffic flow models constitute a tool to study the complex behavior arising in different traffic scenarios. There exists in the literature an enormous quantity of models which represent some aspects of the problem and their origin goes from microscopic to macroscopic approaches. Recently some authors have reviewed the state of arts concerning both points of view [1–6].

Here we will focus our attention on two macroscopic models: the Kerner-Konhäuser macroscopic model [7–9], which is a phenomenological model proposed in close analogy to a Navier-Stokes (N-S) viscous fluid. On the other hand, we will consider a macroscopic model obtained from the kinetic Pavri-Fontana equation [10]; both models contain two equations to describe a traffic scenario and they share the structure.

The Kerner-Konhäuser model [7,9] has been taken as a prototype of hydrodynamic models because it contains the main features of the problem such as the fundamental diagram $V_e(\rho)$ and the values of the relaxation time τ , which are taken according to certain experimental data. On the other hand, the velocity variance Θ_0 and the viscosity η_0 were chosen in a somewhat arbitrary way. It is also known that the simulation of this model under several initial and periodic boundary conditions gives results in which we can see a standard behavior of traffic flow. This model has some problems for certain values of the parameters producing densities bigger than the maximum and negative velocities as were noted in Ref. [9]. In contrast, the kinetic model [10] is based on the Pavri-Fontana kinetic equation [11] with a model for the drivers' desired average velocity; such a model can be classified as a model for aggressive drivers because the desired velocity is bigger than the actual velocity. This model shares the structure with the Kerner-Konhäuser model in the sense that the traffic pressure contains the velocity variance and a kind of viscosity. The simulation results of this model also reproduce the main characteristics of traffic flow as has been discussed in the literature. In both models the vehicle density and the average velocity are taken as relevant variables for vehicles in a one-lane highway with no ramps. The equation of motion for the density is the same and it is given by a conservation equation, while the equation for the average velocity is a balance equation in which the source term will be specified for each model.

First of all, we know that both models admit a solution for a homogeneous steady state characterized by the values of the density and the corresponding velocity, given through the fundamental diagram. However, the observation of simulation results in both models shows that a perturbation from this state creates an inhomogeneous profile which is steady, and we wonder if it is possible the study of such kind of states in a systematic way. This question has been raised in the literature in the context of the study of cluster formation in traffic flow [8]. In particular, the authors in Ref. [8] introduced the methodology appropriate to go from traffic model equations, which are partial differential equations, to ordinary equations by means of a change in the reference frame. Later, Lee *et al.* [12] implemented the scheme to study the steady states in a macroscopic model which comes from an optimal velocity model. In both cases, it is possible to make an analogy with the one-dimensional motion of a particle in a potential field and in the presence of a Stokes friction force. Taking advantage of this analogy, the traffic model equations can be studied with a sensible physical meaning and the theory of dynamical systems can also be used to interpret the results. On the other hand, it is known that the traffic dynamics presents general characteristics such as the presence of the free flow states, synchronized flow, and wide traffic jams [13]. Up to date, all these traffic states are not completely understood, and we think that a first step along these lines is the systematic and complete understanding of the states in the neighborhood of the homogeneous steady states. The analysis in phase space provides us with tools to achieve this goal. In particular, the general characteristics of traffic models, such as their nonlinearity and the presence of dissipation, indicate that this kind of analysis can give a better understanding of the dynamics [14].

The purpose of this work is to do a systematic study of the steady states of the Kerner-Konhäuser and the kinetic models. To begin it, we will consider the problem as seen from a moving reference frame which travels with a constant velocity $-V_g$ and look for the steady states in this new reference system [8,12]. This change in the reference frame allows us to obtain ordinary differential equations which can be studied in the phase space and identify several steady states as well as the orbits in the system. In Sec. II, we first present a general scheme for our study. Section III will be devoted to the Kerner-Konhäuser model, whereas in Sec. IV we will specify the characteristics of the kinetic Navier-Stokes

model. In Sec. V we show some examples of the found orbits in both models and lastly we give some concluding remarks.

II. GENERAL APPROACH

Let us consider in a general way the equations of motion for typical macroscopic traffic models. This means that the analysis will be devoted to models in which we can find a set of equations for averaged quantities such as the density $\rho(x,t)$ and the average velocity $V(x,t)$ of the flow. Some of these models come from a phenomenological approach [7,9]; however, some others have their origin in a kinetic equation [15–17]. The common characteristic of these models is that they share the continuity equation for the density and the structure of the equation of motion for the velocity. Some of them consider three or more equations [9,16,17], but in this work we will only take models which take the density and the average velocity as relevant variables.

To be precise, let us consider a highway with no ramps in such a way that the total number of vehicles remains constant. The equations for the models considered in this work [7,9] can be written in the so-called conservative form as follows:

$$\frac{\partial u}{\partial t} + \frac{\partial F}{\partial x} = S, \quad (1)$$

where

$$u = \begin{pmatrix} \rho \\ \rho V \end{pmatrix}, \quad F \left(u, \frac{\partial u}{\partial x} \right) = \begin{pmatrix} \rho V \\ \rho V^2 + \mathcal{P} \end{pmatrix}. \quad (2)$$

The traffic pressure \mathcal{P} to be considered in this work can be written as

$$\mathcal{P} = \rho \Theta^*(\rho, V) - \eta(\rho, V) \frac{\partial V}{\partial x}, \quad (3)$$

where the quantity Θ^* is the velocity variance which can be a function of the density and the average velocity. The quantity η plays the role of a viscosity and it can also be a function of the averaged variables. On the other hand, the source term $S(u, \frac{\partial u}{\partial x})$ in Eq. (1) is a function of the density, the average velocity, and the velocity gradient. In fact, the source term in the continuity equation for the density vanishes as a consequence of the system conditions, particularly due to the absence of ramps. This means that the density satisfies a conservation equation,

$$\frac{\partial \rho}{\partial t} + \frac{\partial}{\partial x}(\rho V) = 0. \quad (4)$$

Now, let us consider the case where we see the dynamics of the system in a reference frame moving with a constant velocity $-V_g$, in such a way that we make the following change in variable:

$$\xi = x + V_g t, \quad (5)$$

where V_g is constant. In this case Eq. (4) can be immediately integrated in such a way that

$$\rho(V_g + V) = Q_g, \quad \rho = \frac{Q_g}{(V_g + V)}, \quad (6)$$

where Q_g is a constant. Now, the general expression for the traffic pressure (3) is written as

$$\mathcal{P} = \frac{Q_g \Theta^*(V; V_g, Q_g)}{V_g + V} - \eta(V; V_g, Q_g) \frac{dV}{d\xi}. \quad (7)$$

The direct substitution of Eq. (7) in the equation of motion with the change in variable given in Eq. (5) can be written as a second-order ordinary differential equation which has the following general structure:

$$\begin{aligned} \mathcal{M}(V; V_g, Q_g) \frac{d^2 V}{d\xi^2} + \mathcal{D}_1(V; V_g, Q_g) \frac{dV}{d\xi} + \mathcal{D}_2(V; V_g, Q_g) \left(\frac{dV}{d\xi} \right)^2 \\ = \mathcal{F}(V; V_g, Q_g). \end{aligned} \quad (8)$$

The quantities $\mathcal{M}, \mathcal{D}_1, \mathcal{D}_2, \mathcal{F}$ are functions of $(V; V_g, Q_g)$ which will be specified for each model. In all cases, V is the unknown variable while V_g and Q_g are constant parameters. To each V_g and Q_g corresponds a solution $V(\xi)$. The equation just obtained, as it is given in Eq. (8), can be interpreted as the equation of motion for a particle with mass \mathcal{M} , moving in a field of force \mathcal{F} and in the presence of friction terms measured by the coefficients $\mathcal{D}_1, \mathcal{D}_2$. In fact, the field of force can be derived from a kind of potential in such a way that $\mathcal{F} = -\frac{d\mathcal{U}}{dV}$, where the potential \mathcal{U} is also a function of the quantities $(V; V_g, Q_g)$. The points where $\mathcal{F} = 0$ represent critical points of the potential $\mathcal{U}(V; V_g, Q_g)$ and the sign of the derivative $\frac{d\mathcal{F}(V; V_g, Q_g)}{dV} = -K$ at the critical points will tell us if the potential has a maximum or a minimum. In fact, in the model worked out by Lee and co-workers [12], they considered that the potential has a camel's back shape in such a way that there are three extremal points. The stability characteristics of these points determine the kind of traffic dynamics.

We note that in this work we will consider a term proportional to the square of the derivative in the velocity, which is absent in the work of Lee *et al.* [12]. In fact, we will consider it because in the second model we will study here [10], a term like this one appears in a natural way. From the point of view of particle dynamics, this term is equivalent to considering a friction going with the square of the velocity besides the usual linear Stokes term.

A qualitative description can be made in this point; however, at least for the case where the potential has a camel's back structure, such a discussion was made in Ref. [12]. We notice that in Ref. [12], the values of V_g, Q_g are much bigger than the ones we will use in this work. This means that we are working in a different region in the phase space, as we will emphasize in Sec. V.

To analyze the system let us first define dimensionless variables

$$z = \rho_{max} \xi, \quad v = \frac{V}{V_{max}}, \quad v_g = \frac{V_g}{V_{max}}, \quad q_g = \frac{Q_g}{\rho_{max} V_{max}}. \quad (9)$$

Now Eq. (8) can be written as

$$\frac{d^2v}{dz^2} - \Gamma_1(v;v_g,q_g)\frac{dv}{dz} - \Gamma_2(v;v_g,q_g)\left(\frac{dv}{dz}\right)^2 = f(v;v_g,q_g), \tag{10}$$

where

$$-\Gamma_1(v;v_g,q_g) = \frac{D_1}{M},$$

$$-\Gamma_2(v;v_g,q_g) = \frac{D_2}{M},$$

and

$$f(v;v_g,q_g) = \frac{F}{M}.$$

Notice that v is the variable that depends on z , and v_g, q_g are the dimensionless constant parameters.

On the other hand, Eq. (10) can be transformed in a system of two first-order equations when we define the phase space (v, y) and $y = \frac{dv}{dz}$, then

$$\frac{dv}{dz} = f_1, \quad f_1 = y,$$

$$\frac{dy}{dz} = f_2, \quad f_2 = \Gamma_1 y + \Gamma_2 y^2 + f. \tag{11}$$

Here Γ_1, Γ_2, f depend on the velocity v , the constant parameters (v_g, q_g) , and the specific quantities in each model. The properties of the dynamical system defined in Eqs. (11) are determined by the functions f_1, f_2 , and it is clear that the critical points can be calculated from

$$\begin{aligned} f_1(v_c;v_g,q_g) &= 0, \\ f_2(v_c;v_g,q_g) &= 0, \end{aligned} \tag{12}$$

where v_c corresponds to the averaged dimensionless velocity at the critical points. The values for this velocity must be in the range $0 \leq v_c \leq 1$, for the chosen values of $-1 \leq v_g \leq 1$ and $-1 \leq q_g \leq 1$. From Eqs. (11) it is clear that the critical points satisfy the equation $f(v_c;v_g,q_g)=0$ in such a way that their coordinates in phase space are given by $P_c=(v_c, 0)$. We must note that there can be several critical points because the quantity $f(v_c;v_g,q_g)$ can have several roots.

The stability characteristics of the flow can be determined by the linearized dynamical system around each critical point, and for that we need the Jacobian matrix, which is given as

$$J(P_c) = \begin{pmatrix} \left(\frac{\partial f_1}{\partial v}\right)_{P_c} & \left(\frac{\partial f_1}{\partial y}\right)_{P_c} \\ \left(\frac{\partial f_2}{\partial v}\right)_{P_c} & \left(\frac{\partial f_2}{\partial y}\right)_{P_c} \end{pmatrix} = \begin{pmatrix} a_{11}(P_c) & a_{12}(P_c) \\ a_{21}(P_c) & a_{22}(P_c) \end{pmatrix}. \tag{13}$$

A direct calculation shows that $a_{11}=0$, $a_{12}=1$, $a_{21}=\left(\frac{df}{dv}\right)_{v_c} = -K(v_c;v_g,q_g)$, and $a_{22}=\Gamma_1(v_c;v_g,q_g)$.

In fact, we need to calculate the eigenvalues in the Jacobian matrix at each critical point and they are given as

$$L_{\pm} = \frac{1}{2}[\Gamma_1(v_c;v_g,q_g) \pm \sqrt{[\Gamma_1(v_c;v_g,q_g)]^2 - 4K(v_c;v_g,q_g)}]. \tag{14}$$

In order to answer the question about the local stability of the nonlinear system, we apply the Hartman-Gorban theorem that states that critical points, whose corresponding Jacobian matrix has eigenvalues with real part different from zero, have the same behavior as the critical points of the linearized system. These critical points are called hyperbolic points [18,19].

It is well known that when the real part of the eigenvalues is negative we have stability; otherwise, the dynamical system is unstable near the critical point. Notice that if $\Gamma_1(v_c;v_g,q_g) < 0$ and $K(v_c;v_g,q_g) > 0$ the critical points are hyperbolic and stable. When the eigenvalues are real we have a stable node and in the case they are complex we will obtain a stable spiral. In the case where we obtain eigenvalues with negative and positive real parts, the point is said to be a saddle point. It is worth noticing that the linear stability analysis can give us only a qualitative picture near the critical points. Besides the nonlinear term with respect to y in the equation (Γ_2) does not play a role in the linearized analysis. It is not the case for the complete simulations or the construction of orbits in the phase space in the nonlinear case; there, the terms giving place to Γ_2 are relevant. Their order of magnitude is the same as the linear contributions.

Coming back to the analogy with the one-particle motion description, notice that stable nodes correspond to minimum points of the potential. We can also give a physical interpretation of coefficient Γ_1 in terms of the total energy. For that, we will call it the friction linear term, it corresponds to $\Gamma_1 y$, because it is linear with respect to y , while $\Gamma_2 y^2$ will be called the nonlinear friction term. We first note that, in the one-particle analogy, the kinetic energy per unit mass of the particle is given by $\frac{v^2}{2}$, then if we multiply Eq. (10) by $\frac{dv}{dz}$, and recall that the force f is derivable from the potential \mathcal{U} , we obtain

$$\frac{d}{dz}\left(\frac{y^2}{2} + \mathcal{U}\right) = \Gamma_1 y^2 + \Gamma_2 y^3. \tag{15}$$

In the right-hand side of Eq. (15) the terms $\Gamma_1 y^2$ and $\Gamma_2 y^3$ measure the size of the rate of the total energy, then their sign will tell us if there exists dissipation of the total energy in the mechanical system. The first term represented by $\Gamma_1 y^2$ which is positive when the coefficient $\Gamma_1 > 0$ tells us that in this case this term produces energy, whereas when $\Gamma_1 < 0$ there is dissipation. On the other hand, the contribution of the term $\Gamma_2 y^3$ depends on the sign of both factors Γ_2 and y^3 . In the case where in the traffic dynamics only the linear friction term appears, it is the sign of Γ_1 the element which determines dissipation or feedback in the energy. It should be advisable that dissipation of energy and stability around a critical point be consistent with the energy considerations. Then, when the value of the parameter q_g or v_g makes an unstable critical point becomes stable, the energy must be dissipated; otherwise, when a stable critical point becomes unstable the system receives enough energy to escape.

TABLE I. Examples of critical values in the Kerner-Konhäuser model. The third row in each cell gives the stability according to the linear analysis around the critical points. The fourth row gives the characteristics of the potential defined through the force in the equation of motion and the fifth row gives the sign of the friction coefficient in analogy with the one-particle motion. Empty cells imply that there is no value for the critical velocity.

$q_g \mathcal{Q}_g$	$v_g V_g$	$v_0 V_0$	$v_1 V_1$	$v_2 V_2$
0.0952 1600 veh/h	0.1 12 km/h	4.57×10^{-6} 5.84×10^{-4} km/h saddle point maximum $\Gamma_1 < 0$	0.1789 21.46 km/h stable spiral minimum $\Gamma_1 < 0$	0.9327 111.92 km/h saddle point maximum $\Gamma_1 > 0$
0.15 2520 veh/h	0.21 25.2 km/h	4.3×10^{-4} 0.052 km/h saddle point maximum $\Gamma_1 < 0$	0.2783 33.4 km/h unstable spiral minimum $\Gamma_1 > 0$	0.8624 103.49 km/h saddle point maximum $\Gamma_1 > 0$
0.0714 1200 veh/h	-0.1666 -20 km/h		0.4345 52.14 km/h stable spiral minimum $\Gamma_1 < 0$	0.9315 107.42 km/h saddle point maximum $\Gamma_1 > 0$
0.0952 1600 veh/h	-0.11 -13.2 km/h		0.486 58.32 km/h unstable spiral minimum $\Gamma_1 > 0$	0.8952 107.48 km/h saddle point maximum $\Gamma_1 > 0$
0.1074 1804 veh/h	-0.1666 -20 km/h		0.7424 89.08 km/h unstable node minimum $\Gamma_1 > 0$	0.7529 90.34 km/h saddle point maximum $\Gamma_1 > 0$

The second step in the analysis is done with the complete solution of the ordinary differential equations which constitute the dynamical system; in this case, such a set is given in Eqs. (11). The solution of this set of equations is numerical and is given in phase space (v, y) . Obviously, it cannot be done in general and we must go to each specific model.

III. KERNER-KONHÄUSER MODEL

The Kerner-Konhäuser model considers two equations to describe the system: the continuity equation [Eq. (4)] and an equation for the velocity in which the traffic pressure is proposed in analogy with viscous fluid hydrodynamics,

$$\mathcal{P} = \rho \Theta_0 - \eta_0 \frac{\partial V}{\partial x}. \quad (16)$$

Hence, the equation describing the time evolution of the velocity is given as

$$\frac{\partial V}{\partial t} + V \frac{\partial V}{\partial x} = - \frac{\Theta_0}{\rho} \frac{\partial \rho}{\partial x} + \frac{\eta_0}{\rho} \frac{\partial^2 V}{\partial x^2} + \frac{1}{\tau} [V_e(\rho) - V], \quad (17)$$

where both Θ_0, η_0 and the individual relaxation time τ are constants. This model is a phenomenological one, since it was proposed in analogy with the Navier-Stokes equation in a fluid characterized by the viscosity η_0 and a kind of hydrostatic pressure which is measured through the first term in the traffic pressure. The numerical values of these parameters are somewhat arbitrary, but it is well known that in this case the equations of motion can be simulated and they give a convergent solution with a well-behaved profile in the density and the velocity, at least in some regions of the values of the parameters. The fundamental diagram $V_e(\rho)$ which gives the relation between the so-called equilibrium velocity and the density is also given and it is taken from experimental data [7].

We now apply the results in Sec. II to the Kerner-Konhäuser model, where we identify the source in Eq. (1) as

$$S(u) = \begin{pmatrix} 0 \\ \frac{1}{\tau} [V_e(V) - V] \end{pmatrix}. \quad (18)$$

With the change in variable proposed in Eq. (5), the substitution of the density according to Eq. (6) and taking into account the definition of the dimensionless variables (9), we obtain

$$\frac{d^2v}{dz^2} - a \left[1 - \frac{\theta_0}{(v+v_g)^2} \right] \frac{dv}{dz} + b \left(\frac{v_e(v) - v}{v+v_g} \right) = 0, \quad (19)$$

where we have defined some dimensionless quantities special for this model as

$$v_e(v) = \frac{V_e(V)}{V_{max}}, \quad \theta_0 = \frac{\Theta_0}{V_{max}^2}, \quad a = \frac{Q_g}{\rho_{max} \eta_0},$$

$$b = \frac{Q_g}{\rho_{max}^2 \eta_0 \tau V_{max}}. \quad (20)$$

Now, the corresponding dynamical system can be written as

$$\frac{dv}{dz} = y,$$

$$\frac{dy}{dz} = a \left[1 - \frac{\theta_0}{(v+v_g)^2} \right] y - b \left(\frac{v_e(v) - v}{v+v_g} \right). \quad (21)$$

Comparing with Eq. (11) we obtain

$$f_1 = y, \quad f_2 = a \left[1 - \frac{\theta_0}{(v+v_g)^2} \right] y - b \left(\frac{v_e(v) - v}{v+v_g} \right), \quad (22)$$

and the coordinates of the critical points will be given as $(v_c, 0)$ such that

$$v_e(v_c) - v_c = 0. \quad (23)$$

It is a direct calculation to show that the elements of the Jacobian matrix [Eq. (13)] depend on the parameters of the model and the solution v_c which determines the coordinates of the critical points; hence,

$$\Gamma_1(P_c) = a \left[1 - \frac{\theta_0}{(v_c + v_g)^2} \right],$$

$$-K(P_c) = \frac{b}{(v_c + v_g)} \left[1 - \left(\frac{dv_e}{dv} \right)_{v_c} \right]. \quad (24)$$

Obviously an explicit calculation requires numerical values for all parameters and the fundamental diagram; in this case, we have taken the following values [9]:

$$\rho_{max} = 140 \text{ veh/km}, \quad V_{max} = 120 \text{ km/h}, \quad \tau = 30 \text{ s},$$

$$\Theta_0 = (45 \text{ km/h})^2, \quad \eta_0 = 600 \text{ km/h},$$

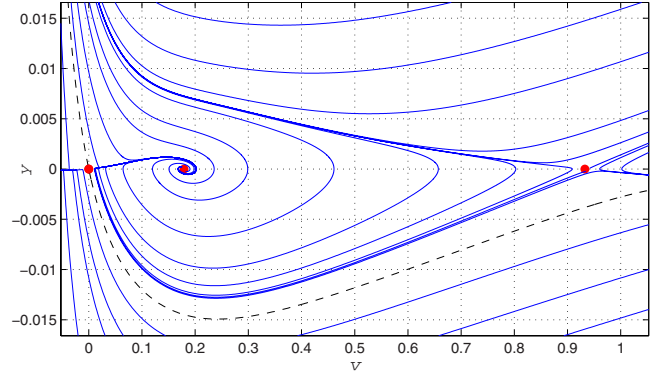


FIG. 1. (Color online) Orbits in phase plane for the Kerner-Konhäuser model for $q_g=0.0952$ and $v_g=0.1$. The values corresponding to the critical points are in the first row of Table I. There is a heteroclinic path that links the first to the second critical point, and the dashed line corresponds to the separatrix.

$$\frac{V_e}{V_{max}} = -3.72 \times 10^{-6} + \left[1 + \exp\left(\frac{\frac{\rho}{\rho_{max}} - 0.25}{0.06} \right) \right]^{-1}, \quad (25)$$

where the density ρ is measured in vehicles/km (veh/km). Also, the values for q_g and v_g must be given; however, they can be positive or negative provided the density is positive in Eq. (6). For each pair of values (q_g, v_g) we will obtain different critical points.

Table I represents only some values for critical points corresponding to certain values of the parameters q_g and v_g ; however, we can notice some stability characteristics of the model. When the quantities q_g, v_g are positive, we have three to none critical points depending on the values of these parameters, while for $q_g > 0$ and $v_g < 0$ we obtained two to none critical points. When $q_g < 0$ (not shown in Table I) we just obtained one critical point $v_c > |v_g|$ which corresponds to a stable spiral. In the first example we obtain three critical points: at the saddle points v_0 and v_2 the potential attains a maximum value, whereas the point v_1 is stable. In the second case, the minimum of the potential v_1 is an unstable spiral and points v_0, v_2 are saddle points where the potential attains a maximum value. The last three data correspond to $q_g > 0$ and $v_g < 0$; for these particular cases, we have two critical points. Point v_2 corresponds to a maximum in the potential and it is a saddle point. The critical point in v_1 is a minimum in the potential, but its stability characteristics changes according to the values of v_g, q_g . Notice that the stability region is small; a slight change in the parameters q_g, v_g causes that the stable point becomes unstable.

From these data it is possible to have a qualitative analysis as it was done by Lee *et al.* [12]. To go deeper in the analysis it is necessary to construct the orbits in the phase space (v, y) . The construction of orbits is based on the numerical solution for the complete dynamical system, and we will give here some examples. In Fig. 1 we have the orbits for the values in the first row in Table I. In this case there is a heteroclinic path that links v_0 to v_1 ; on the other hand, there is neither a heteroclinic orbit between the critical points

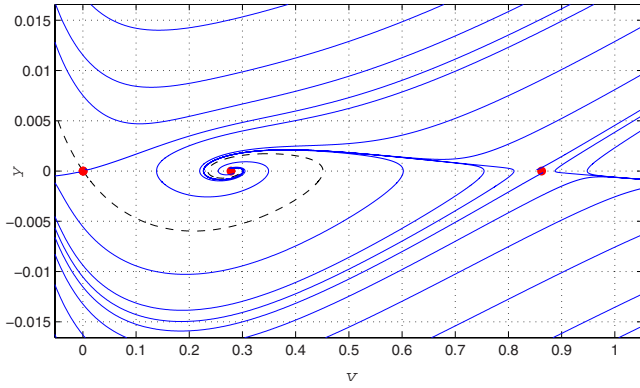


FIG. 2. (Color online) Orbits in phase plane for $q_g=0.15$ and $v_g=0.21$. There are three unstable critical points, whose values are listed in the second row of Table I. There is a heteroclinic orbit that links the second to the third critical point, and the dashed orbit corresponds to the separatrix.

$v_0 \rightarrow v_2$ nor $v_1 \rightarrow v_2$. We notice that the existence of the heteroclinic orbit linking v_0 and v_1 means that the velocity as a function of the variable z goes from a homogeneous steady state v_0 to a new homogeneous steady state v_1 , and the corresponding solution corresponds to a nonhomogeneous profile. This solution starts in v_0 , has a small oscillation, and ends in v_1 . Figure 1 shows in a clear way the stability characteristics of points, v_1 as a stable spiral and we have a saddle for v_2 . Figure 2 shows the orbits for the second row of Table I, although we have three critical points: v_0 and v_2 are saddle points, whereas v_1 is an unstable node. There is a heteroclinic trajectory linking $v_1 \rightarrow v_2$. In this case the presence of the heteroclinic orbit tells us that the system goes from the homogeneous steady state characterized by v_1 to a new state v_2 ; however, the inhomogeneous velocity profile as a function of variable z oscillates and then goes smoothly to v_2 .

In Fig. 3 we show for $q_g=0.0952$ (1600 veh/h) and $v_g=0.2$ (24 km/h) a case where there is only one critical point at $v_1=0.91459$ (109 km/h) which is a saddle. In Fig. 4 we have the orbits in the phase plane in the case where we have taken $q_g > 0$ and $v_g < 0$. The first observation in this case is that we have a discontinuity in the force f and the friction coefficient Γ_1 for $v=|v_g|$; however, when $v > |v_g|$ we obtain

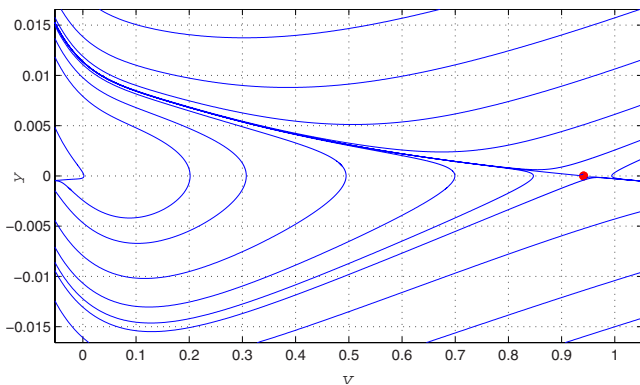


FIG. 3. (Color online) Orbits in phase plane for $q_g=0.0952$ and $v_g=0.2$. There is only one critical point which is a saddle.

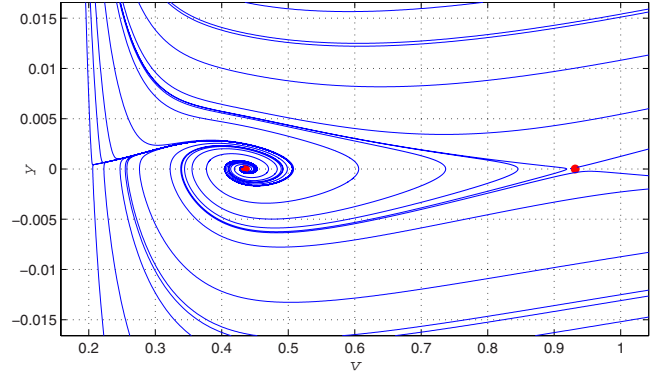


FIG. 4. (Color online) Orbits in phase plane for $q_g=0.0714$ and $v_g=-0.1666$. There are two critical points, whose values are listed in the third row of Table I; the first one is a stable spiral while the other is a saddle.

two critical points v_1 and v_2 . Now there can be a heteroclinic orbit $v_2 \rightarrow v_1$, corresponding to a velocity profile which goes smoothly from v_2 , then oscillates, and ends in v_1 . Such a profile corresponds to an inhomogeneous solution v vs z .

In Fig. 5 it is shown the phase plane for $v_g=-0.1$ (-12 km/h) and $q_g=0.0952$ (1600 veh/h). The most remarkable property in this case is that it seems to appear a limit cycle surrounding the stable critical point v_1 . In this case the inhomogeneous profile corresponding to the limit cycle becomes periodic. The orbits inside the limit cycle approach the stable critical point and the orbits outside the limit cycle go far apart. Notice that a small change in v_g causes a change in the stability region, as it shown in example 4 of Table I: for $v_g=-0.11$, v_1 becomes unstable because $\Gamma_1(v_1)$ becomes positive.

In Fig. 6 we see an example of the orbits when $q_g > 0$, $v_g < 0$, and the limit cycle is not present. In this case there are two critical points very close to each other (see the fifth row of Table I); v_2 is a saddle point and although the potential attains its minimum value at v_1 , it is an unstable node due to the fact that $\Gamma_1 > 0$.

These examples have shown the orbits in different cases and we can compare with the qualitative analysis done by Lee *et al.* [12], where they identified several regions in the

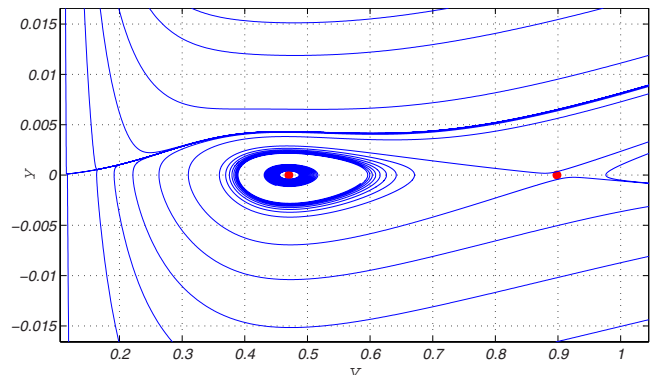


FIG. 5. (Color online) Orbits in the phase space for $q_g=0.0952$ and $v_g=-0.1$. There are two critical points. The first one is stable while the other is a saddle point.

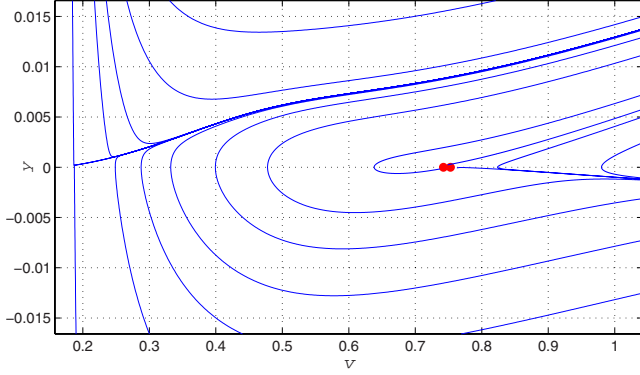


FIG. 6. (Color online) Orbits for $q_g=0.107$ and $v_g=-0.166$. There are two unstable critical points whose values are listed in the fifth row of Table I.

phase plane according to the characteristics of the orbits. We notice that in the analysis of Lee *et al.* [12] they only considered the cases where $v_g > 0$. It is worth to notice that v_g can be identified with the velocity of propagation of a cluster (see [8]), which can propagate upstream or downstream, so the case $v_g < 0$ has physical meaning. Obviously it is possible to give more examples; however, the dependence of orbits with the values in q_g and v_g makes an exhaustive search, somewhat cumbersome.

IV. KINETIC NAVIER-STOKES-LIKE MODEL

After the discussion of the phenomenological model introduced by Kerner and Konhäuser [7], we will study a model called kinetic N-S [10]. This model has its origin in the Pavari-Fontana kinetic equation [11] where a special form for the averaged desired velocity of drivers is introduced. Then the exact solution for the homogeneous steady state is obtained and the maximization of the informational entropy allowed us the construction of a local distribution function in which the local density and the velocity appear in an explicit way. This distribution function was the basis to develop a perturbation method to find the traffic pressure in terms of a collective relaxation time. As a result it was obtained an expression for the traffic pressure with the structure of Eq. (3) where $\Theta^*(\rho, V) = \frac{V^2}{\alpha}$ and the viscosity $\eta(\rho, V) = \frac{\rho V^2 \tau^*}{\alpha}$. The parameter α is a constant at the low-density region, with a value which can be obtained from experimental data [20]. In fact, $\frac{1}{\alpha}$ is the so-called prefactor of the variance. It is a standard procedure to obtain, from the Pavari-Fontana equation, the time evolution for the density and the velocity. In fact, the density satisfies the continuity equation (4) and the velocity equation can be written as

$$\frac{\partial V}{\partial t} + V \frac{\partial V}{\partial x} = -\frac{1}{\rho} \frac{\partial \mathcal{P}}{\partial x} + \frac{1}{\tau} (W - V) - (1-p)\mathcal{P}, \quad (26)$$

where p is the probability of overtaken and the traffic pressure is now given as

$$\mathcal{P} = \frac{\rho V^2}{\alpha} \left(1 - \tau^* \frac{\partial V}{\partial x} \right). \quad (27)$$

In Eq. (26), $W = \omega V$ is the averaged desired velocity of drivers, and in this model it is proposed with a parameter ω which measures the average aggressiveness of drivers. The quantity α in Eq. (27) is a dimensionless quantity determined by the experimental data [20] and it is given by

$$\alpha = \frac{\rho_e (1-p) \tau V_e}{\omega - 1}, \quad \tau^* = 2\tau_0 \frac{1 + \alpha}{\alpha}, \quad (28)$$

where τ_0 is a collective relaxation time introduced in the kinetic method [10] which must be greater than the individual relaxation time τ , lastly, V_e is related to the density ρ through the fundamental diagram given phenomenologically as usual [see Eq. (25)].

Now the equation of motion is written in terms of the variable ξ as defined in Eq. (5) and the result is written as in Eq. (8). When we substitute the dimensionless variables as defined in Eq. (9) and the dimensionless times $T_c = \tau^* \rho_{max} V_{max}$, $T_i = \tau \rho_{max} V_{max}$, we can write the complete equation for the velocity as

$$\begin{aligned} \frac{d^2 v(z)}{dz^2} - \left\{ \frac{\alpha[v(z) + v_g]}{T_c v^2(z)} - \frac{(1-p)q_g}{v(z) + v_g} + \frac{v(z) + 2v_g}{v(z)[v(z) + v_g]} \right\} \frac{dv(z)}{dz} \\ + \frac{v(z) + 2v_g}{v(z)[v(z) + v_g]} \left[\frac{dv(z)}{dz} \right]^2 + \frac{\alpha(\omega - 1)}{T_c T_i v(z)} - \frac{(1-p)q_g}{T_c [v(z) + v_g]} \\ = 0. \end{aligned} \quad (29)$$

We can identify the functions in the system given in Eqs. (11),

$$\Gamma_1(v; v_g, q_g) = \frac{\alpha(v + v_g)}{T_c v^2} - \frac{(1-p)q_g}{v + v_g} + \frac{v + 2v_g}{T_c v(v + v_g)}, \quad (30)$$

$$\Gamma_2(v; v_g, q_g) = -\frac{v + 2v_g}{v(v + v_g)}, \quad (31)$$

$$f(v; v_g, q_g) = \frac{(1-p)q_g}{T_c(v + v_g)} - \frac{\alpha(\omega - 1)}{T_c T_i v}, \quad (32)$$

and the coordinates of the critical points can be found with the condition $f(v; v_g, q_g) = 0$. In the calculation of the critical points, it is important to notice that f depends on the parameters in the model through α which is given in Eq. (28) and in terms of the fundamental diagram $V_e(V)$, in such a way that we can eliminate the parameter ω . The result of this procedure allows us to write the force in the following manner:

$$f(v; v_g, q_g) = \frac{(1-p)q_g}{T_c(v + v_g)} \left(1 - \frac{v_e(v)}{v} \right). \quad (33)$$

In this equation it is clear that the force vanishes when Eq. (23) is satisfied. As a result we obtain that the critical points in this model are given by the same condition as in the

TABLE II. Examples of critical values in the Navier-Stokes-like model. The meaning of each row is the same as in Table I.

q_g Q_g	v_g V_g	v_0 V_0	v_1 V_1	v_2 V_2
0.0952 1600 veh/h	0.1 12 km/h	4.57×10^{-6} 5.84×10^{-4} km/h saddle point maximum $\Gamma_1 > 0$	0.1789 21.46 km/h unstable node minimum $\Gamma_1 > 0$	0.9327 111.92 km/h saddle point maximum $\Gamma_1 > 0$
0.15 2520 veh/h	0.21 25.2 km/h	4.3×10^{-4} 0.052 km/h saddle point maximum $\Gamma_1 > 0$	0.2783 33.4 km/h unstable node minimum $\Gamma_1 > 0$	0.8624 103.49 km/h saddle point maximum $\Gamma_1 > 0$
0.0952 1600 veh/h	-0.1 -12 km/h		0.4702 56.42 km/h stable spiral minimum $\Gamma_1 < 0$	0.8984 107.80 km/h saddle point maximum $\Gamma_1 > 0$
0.1072 1800 veh/h	-0.1 -12 km/h		0.55095 66.14 km/h stable spiral minimum $\Gamma_1 < 0$	0.86004 103.21 km/h saddle point maximum $\Gamma_1 > 0$
0.119 2000 veh/h	-0.1 -12 km/h		0.68555 82.27 km/h unstable spiral minimum $\Gamma_1 > 0$	0.7663 91.96 km/h saddle point maximum $\Gamma_1 > 0$

Kerner-Konhäuser model; this means that in both models the critical points are the same.

The quantity $f(v; v_g, q_g)$ represents the force per unit mass in the analogy with the motion of a particle, and we notice here that the force in both models is not the same, although the points where it vanishes coincide. In fact, in the kinetic Navier-Stokes-like model the force depends on the probability of overtaking $(1-p)$ which can be taken from experimental data; here we will take it as $(1-p) = \frac{\rho}{\rho_{max}} = \frac{q_g}{v+v_g}$, a factor which is not present in the Kerner-Konhäuser model. It is worth noticing that the stability analysis around the critical points is a linear one, which means that the nonlinear term with respect to y present in this model, which is proportional to $\Gamma_2(v; v_g, q_g)$, does not play any role. The results coming from the linear analysis are valid only in a neighborhood of each critical point, and they do not give a definite answer about the global stability in the system. The construction of orbits in phase space as well as the simulation results depends on Γ_2 in an explicit and important way.

In Table II we show some examples of values for the

critical points, their stability, the characteristics of the potential, and the sign of the Stokes friction term. The first two rows correspond to $q_g > 0$ and $v_g > 0$. In both cases there are three critical points but unlike the Kerner-Konhäuser model, none of them are stable for this model; v_0 and v_2 correspond to maximums of the potential and are saddle points while point v_1 corresponds to a minimum in the potential and it is an unstable node. Consistently with the analysis in terms of the energy rate we found that Γ_1 evaluated in v_1 is positive. In the case where $q_g > 0$ and $v_g < 0$, there are only two critical points after the singularity of the force $v > |v_g|$, as it occurred in the Kerner-Konhäuser model. The orbits in phase space can be constructed with the complete solution of the dynamical system given through Eqs. (11) and (30) and taking specific values for v_g, q_g . In this case the relaxation times are taken as $\tau = 30$ s and $\frac{\tau}{\tau} = 10$. The value for the quotient in relaxation times deserves some comments; first of all we recall that τ is an individual relaxation time which measures the individual disposition of drivers. Second, the collective relaxation time τ^* represents an average collective time, which in the development of the model has been taken as

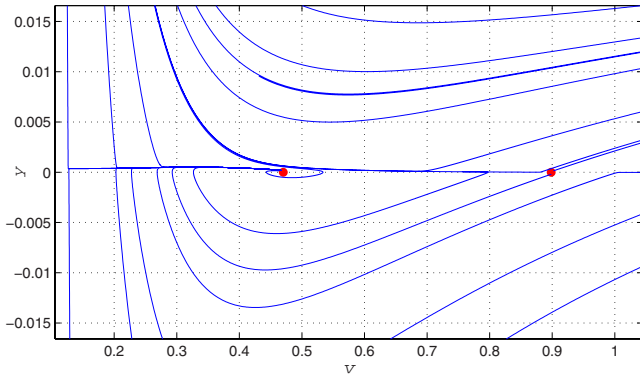


FIG. 7. (Color online) Orbits for the kinetic Navier-Stokes-like model for $q_g=0.0952$ and $v_g=-0.1$. There are two critical points whose values are listed in the third row of Table II. The first one is a stable spiral while the second one is a saddle point.

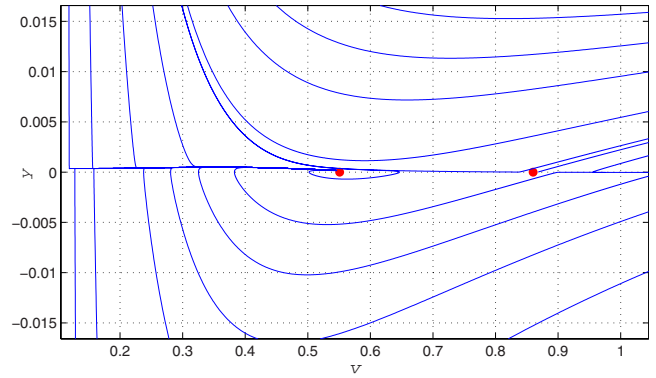


FIG. 8. (Color online) Orbits in phase plane for $q_g=0.1072$ and $v_g=-0.1$. There are two critical points whose values appear in the fourth row of Table II. The first one is a stable spiral while the other is a saddle point.

greater than the individual relaxation time. Third, we have found that the quotient between relaxation times plays an important role in the stability of system. In fact, if we choose a small quotient (~ 1), we do not obtain critical points and the simulation of the model for usual initial conditions cannot be obtained. As an additional remark, recently it was shown by means of the usual Chapman-Enskog expansion in the reduced Paveri-Fontana equation that the collective relaxation time can be determined in terms of the ω value and τ by means of the expression $\tau_0 = \frac{\tau}{2(\omega-1)}$ [21]. In this case the quotient is always greater than 1 and near 10, as we are choosing.

Also, it is important to mention that the scale of the values for the derivative in the velocity as well as the values for the force are different when compared with the corresponding terms in the Kerner-Konhuser model. This characteristic makes the construction of orbits in phase space somewhat difficult to present in graphics mainly for the data in the first and the second rows in Table II, which correspond to values $q_g > 0, v_g > 0$; however, when we have $q_g > 0, v_g < 0$ we can observe the two critical points. Those are located in $y=0$ as it should be; according to the values in v_g , we see that the critical values become closer to each other. This feature is seen in Figs. 7 and 8; besides in these figures we can see that point v_1 corresponds to a stable spiral whereas in Fig. 9 the critical point v_1 is an unstable spiral. In this case it is important to notice that the value q_g plays the role of a bifurcation parameter in the system. When the q_g value grows there are not critical points. So far, we have not found a limit cycle as it happened in the Kerner-Konhuser model. It means that, in this model, either we do not have one limit cycle or it is in a different region in phase space.

V. CONCLUDING REMARKS

The study of steady states in traffic flow is a problem of great importance in the dynamics of such systems. First we wonder if the homogeneous steady states, which are apparent in traffic flow, are stable or unstable. Besides, nonhomogeneous steady states may appear in real traffic, for example, we can think in synchronized flow or wide jams as a kind of

steady states. This is a question which to our knowledge has not a definite answer. On the other hand, from the point of view of macroscopic models, we can ask ourselves if those models present stable nonhomogeneous steady states. In the search of such steady states the first step to be done is a systematic study of typical models in which we can solve some of the questions we have just asked. In the literature [8–12] there has been some interest in this subject; in particular [8] introduced the appropriate methodology while Lee *et al.* [12] applied it to study the steady states for an optimal velocity model.

The models we have developed in this work share the same structure as the ones indicated previously and in both cases the analogy with the motion of a particle gives an interpretation of quantities containing the traffic model parameters. In fact, both models can be described in terms of a particle submerged in a potential field with friction forces; in the Kerner-Konhuser model we have a linear friction term with respect to y , while in the kinetic Navier-Stokes model we also have a nonlinear friction term. It is a remarkable property that in both models the critical points are the same, meaning that the homogeneous steady states are also the same. Just to be precise, for a given set of values v_g, q_g those critical points in the dynamical system are fixed in phase space. Hence, the velocity v and its derivative y are fixed;

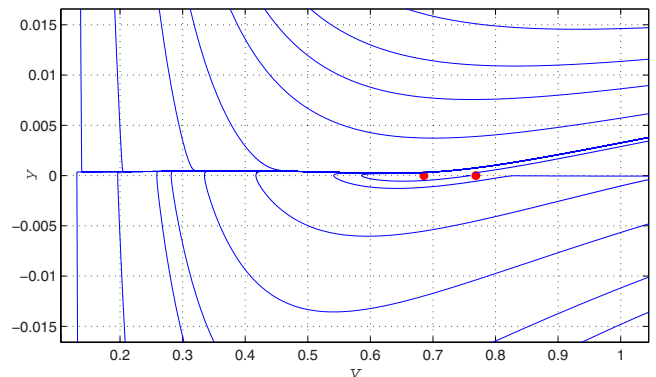


FIG. 9. (Color online) Orbits in phase plane for $q_g=0.119$ and $v_g=-0.1$. There are two unstable critical points whose values appear in the fifth row of Table II.

consequently, in these states the density ρ has also a fixed value, all of them being constant in position and time along the highway. On the other hand, the states near those critical points correspond to traffic states tending to homogeneous steady state in the case of a stable critical point; otherwise, they go far apart. In the context of the particle motion, stability is obtained when the total energy of the particle is dissipated by friction and this is given by the sign of Γ_1 . The unstable case can be obtained near a maximum in the potential and when there are some factors which make that energy grows. Also, a stable state can become unstable if we have an overload in the total energy. The potential field in the macroscopic models depends on the fundamental diagram; in our case the fundamental diagram chosen drives to a potential with three, two, or one critical point, although there are cases where the critical points do not exist. Accordingly, in the case of three critical points we have obtained two maximums and one minimum for $v_g > 0$, $q_g > 0$; a negative sign in the friction coefficient Γ_1 drives to energy dissipation and we can see that stable points correspond to a negative coefficient. Saddle points are associated with positive friction coefficient, a characteristic which is consistent with the description of the particle motion.

When we choose $q_g > 0$, $v_g < 0$ there exists a discontinuity in the functions; however, it is possible to analyze the dynamical system in a region where the continuity of functions is present. The potential field in this case has two critical points; in the Kerner-Konhäuser model the minimum can be stable or unstable, depending on the sign of Γ_1 , while the maximums are unstable. It is worth noticing that the stability of a critical point depends on both factors the characteristics of the potential and the friction coefficient. The values of q_g and v_g play the role of bifurcation parameters in the system. Also, notice that the sign in the friction coefficient corresponds to the qualitative picture we just mentioned above. In fact, this case corresponds to the one analyzed by Kerner and Konhäuser [8] to study the formation of clusters in a closed road. This is also the case in the kinetic Navier-Stokes model.

In our work we have constructed explicitly the orbits in phase space for several cases. It is particularly important that

we have found signs of the presence of limit cycles in phase space. They appear for some values of v_g, q_g and the friction coefficient $\Gamma_1 < 0$ as it should be. Also, in the work of Lee *et al.* [12] the limit cycles can appear for some values of the parameters; in this sense we have found numerically certain properties similar to their case. It must be noted that in our work the orbits in phase space are calculated numerically and they correspond to some qualitative cases as reported by Lee *et al.* The values we have chosen to calculate the orbits correspond to the free traffic region in the fundamental diagram. When we compared with the work of Lee *et al.* we found that they were working in a region different than ours; their region corresponds to bigger values for q_g and v_g , making the quantitative comparison a nonsense work.

As another piece of the conclusions of our work we can make a comparison between the two macroscopic models we have worked out. First of all, both models share the structure in the equations of motion, and the critical points are the same. It is not the case with respect to the values of the potential field, the force, the stability of the critical points, and of course the orbits in phase space. Let us now go into the discussion of the details; the Kerner-Konhäuser model is a phenomenological one in which the parameters such as the viscosity and the variance are chosen arbitrarily, whereas the kinetic Navier-Stokes model is based on a kinetic equation. It has only one free parameter which is called the collective relaxation time; however, the viscosity and the variance are determined by the dynamics. The validity region for each model is different; the first model can be applied for any value of the density, whereas in the second the density must be in a dilute region. This fact was the cause to choose the analysis in the free traffic regime. The second model presents unstable critical points except in the case where we have $q_g > 0$, $v_g < 0$; however, the stable critical point occurs for velocity values near the maximum velocity. It is worth mentioning that the simulation of both models can be done; the results converge and they present a kind of permanent profiles in the density and the velocity. Certainly, the resulting profiles look different but in both cases they have the general characteristics of traffic flow.

-
- [1] D. Helbing, *Rev. Mod. Phys.* **73**, 1067 (2001).
 [2] D. Chowdhury, L. Santen, and A. Schadschneider, *Phys. Rep.* **329**, 199 (2000).
 [3] S. Maerivoet and B. De Moor, *Phys. Rep.* **419**, 1 (2005).
 [4] S. P. Hoogendoorn and P. H. L. Bovy, *Proc. Inst. Mech. Eng. Part I: J. Syst. Contr. Eng.* **215**, 283 (2001).
 [5] T. Nagatani, *Rep. Prog. Phys.* **65**, 1331 (2002).
 [6] R. M. Velasco and P. Saavedra, *Qual. Theory Dyn. Syst.* **7**, 237 (2008).
 [7] B. S. Kerner and P. Konhäuser, *Phys. Rev. E* **48**, R2335 (1993).
 [8] B. S. Kerner and P. Konhäuser, *Phys. Rev. E* **50**, 54 (1994).
 [9] D. Helbing, *Phys. Rev. E* **51**, 3164 (1995).
 [10] R. M. Velasco and W. Marques, Jr., *Phys. Rev. E* **72**, 046102 (2005).
 [11] S. L. Paveri-Fontana, *Transp. Res.* **9**, 225 (1975).
 [12] H. K. Lee, H. W. Lee, and D. Kim, *Phys. Rev. E* **69**, 016118 (2004).
 [13] B. S. Kerner, *The Physics of Traffic* (Springer, New York, 2004).
 [14] P. G. Drazin and R. S. Johnson, *Solitons: An Introduction* (Cambridge University Press, Cambridge, England, 1990).
 [15] D. Helbing and M. Treiber, *Granular Matter* **1**, 21 (1998).
 [16] C. Wagner, C. Hoffmann, R. Sollacher, J. Wagenhuber, and B. Schürmann, *Phys. Rev. E* **54**, 5073 (1996).
 [17] A. R. Méndez and R. M. Velasco, *Transp. Res., Part B: Methodol.* **42**, 782 (2008).
 [18] D. W. Jordan and P. Smith, *Nonlinear Ordinary Differential Equations* (Oxford University Press, New York, 1999).
 [19] S. Wiggins, *Introduction to Applied Nonlinear Dynamical Systems and Chaos* (Springer, New York, 1990).
 [20] V. Shvetsov and D. Helbing, *Phys. Rev. E* **59**, 6328 (1999).
 [21] W. Marques (private communication).